Inhibition of the FKBP family of peptidyl prolyl isomerases induces abortive translocation and degradation of the cellular prion protein

Pawel Stocki[a,†], Maxime Sawicki[a,†], Charles E. Mays[b], Seo Jung Hong[a], Daniel C. Chapman[c], David Westaway[b,d], and David B. Williams[a,c,*]
[a]Department of Biochemistry and [c]Department of Immunology, University of Toronto, Toronto, ON M5S 1A8, Canada; [b]Centre for Prions and Protein Folding Diseases and [d]Division of Neurology and Departments of Chemistry and Biochemistry, University of Alberta, Edmonton, AB T6G 2M8, Canada

ABSTRACT Prion diseases are fatal neurodegenerative disorders for which there is no effective treatment. Because the cellular prion protein (PrP^C) is required for propagation of the infectious scrapie form of the protein, one therapeutic strategy is to reduce PrP^C expression. Recently FK506, an inhibitor of the FKBP family of peptidyl prolyl isomerases, was shown to increase survival in animal models of prion disease, with proposed mechanisms including calcineurin inhibition, induction of autophagy, and reduced PrP^C expression. We show that FK506 treatment results in a profound reduction in PrP^C expression due to a defect in the translocation of PrP^C into the endoplasmic reticulum with subsequent degradation by the proteasome. These phenotypes could be bypassed by replacing the PrP^C signal sequence with that of prolactin or osteopontin. In mouse cells, depletion of ER luminal FKBP10 was almost as potent as FK506 in attenuating expression of PrP^C. However, this occurred at a later stage, after translocation of PrP^C into the ER. Both FK506 treatment and FKBP10 depletion were effective in reducing PrP^{Sc} propagation in cell models. These findings show the involvement of FKBP proteins at different stages of PrP^C biogenesis and identify FKBP10 as a potential therapeutic target for the treatment of prion diseases.

INTRODUCTION

The cellular prion protein (PrP^C) plays a pivotal role in the development of a number of incurable and debilitating neurodegenerative diseases, known as prion diseases, which include Creutzfeldt–Jakob disease in humans, bovine spongiform encephalopathy, and chronic wasting disease in deer and elk. These diseases are characterized by the accumulation in lymphoid tissue and brain of a misfolded oligomer of PrP^C termed PrP-scrapie (PrP^{Sc}). Pioneering work by Prusiner and coworkers identified PrP^{Sc} as the predominant component of

the transmissible agent (Prusiner, 1982; Prusiner et al., 1983). In the current model of PrP^{Sc} propagation, direct contact between PrP^{Sc} and PrP^C results in a templated change of the latter to the PrP^{Sc} conformer with further oligomerization that often leads to the formation of amyloid fibrils. Subsequent fibril fragmentation and secondary nucleation result in self-propagating exponential growth of amyloids (Masel et al., 1999; Knowles et al., 2009). Of importance, it has been shown that host PrP^C expression is a prerequisite for prion disease development (Brandner et al., 1996; Mallucci et al., 2003) and that the presence of the glycosylphatidylinisotol (GPI)-membrane anchor of PrP contributes to the development of clinical symptoms of scrapie (Chesebro et al., 2005).

Given that prion diseases are fatal and incurable, there is intense interest in identifying drugs that impede prion propagation. Many candidates have been identified, such as polyanionic compounds, polyene antibiotics, tetrapyrrolic, tetracyclic, and tricyclic compounds, Congo red and analogues, and β-sheet breaker peptides (reviewed in Trevitt et al., 2006). Several of these act by binding directly to either PrP^C or PrP^{Sc}. However, their utility is limited due to poor efficacy, inability to cross the blood–brain barrier, or the need

to use them at very early, asymptomatic stages of prion infection. An alternative approach of reducing PrP^C expression and thereby limiting PrP^{Sc} propagation has been more successful. This was first demonstrated in Prnp$^{-/-}$ mice, which lack PrP^C and are resistant to PrP^{Sc} infection and subsequent disease development (Bueler et al., 1993). Similarly, conditional neuronal knockout of PrP^C expression had no major deleterious effects in mice and prevented disease progression, even reversing pathology when the knockout was performed 8 wk after infection (Mallucci et al., 2003). Lentiviral-mediated RNA interference has also been used therapeutically to reduce PrP^C expression in brains of prion-infected mice and reduce subsequent disease pathology and extend survival time (White et al., 2008). Therefore reducing PrP^C expression appears to be a viable therapeutic approach for the treatment of prion disease. A recent screen for human-approved drugs that reduce cell surface PrP^C level by >50% identified nine such compounds, including the immunosuppressive drug tacrolimus, also known as FK506 (Karapetyan et al., 2013).

FK506 binds to the FK506-binding protein (FKBP) family of peptidyl prolyl isomerases and inhibits their enzymatic activities (Barik, 2006). However, its immunosuppressive effect arises from the binding of FK506-FKBP complexes to calcineurin, inhibiting its phosphatase activity and resulting in inactivation of the nuclear factor of activated T-cells that is required for T-cell activation (Flanagan et al., 1991; Liu et al., 1991). Several recent studies examined the effect of FK506 treatment on PrP^C or PrP^{Sc} levels in cells and on disease progression in prion-infected mice. Mukherjee et al. (2010) showed that FK506 protected mouse N2a neuroblastoma cells against the toxic effects of exogenously added PrP^{Sc} and also reduced the severity of disease and increased survival time in prion-infected mice. These effects were attributed to FK506 inhibition of the elevated calcineurin activity observed in both infected cells and mouse brain. Other studies found that FK506 treatment reduced PrP^C expression in mouse PK1 neuroblastoma cells and inhibited PrP^{Sc} replication, but no increase in survival was observed in prion-infected mice (Karapetyan et al., 2013). The reduced PrP^C expression occurred posttranscriptionally, but enhanced autophagy was ruled out as a possible mechanism. In contrast, Nakagaki et al. (2013) observed that FK506 treatment of mouse N2a58 neuroblastoma cells modestly reduced PrP^C levels, activated autophagy, and strongly impaired PrP^{Sc} propagation. It also reduced pathological changes and increased survival times in mice infected with the Fukuoka-1 or hamster 263K prion strains. Therefore, although promising results have been obtained with this human-approved drug, there are conflicting views as to how it impairs prion propagation and essentially no information on the mechanism by which it reduces PrP^C expression.

PrP^C is a GPI-anchored cell surface protein existing in a number of isoforms. It has one disulfide bond and two N-glycosylation sites, which are used with different efficiencies, resulting in three glycoforms: nonglycosylated, monoglycosylated at either of the two N-linked sites, or diglycosylated. PrP^C is targeted to the endoplasmic reticulum (ER) by its N-terminal signal peptide, but ~10–20% is inefficiently recognized by the translocation machinery, resulting in abortive translocation and redirection into the cytosol for subsequent degradation by the proteasome (Drisaldi et al., 2003; Rane et al., 2004; Kang et al., 2006). The abortive translocation has been proposed to be a part of a regulatory mechanism acting to lessen the burden of translocation of nonessential and potentially misfolding-prone proteins upon stress conditions (Kang et al., 2006). After translocation, the majority of PrP^C undergoes GPI modification within the ER, transport through the canonical secretory pathway, and expression at the cell surface. Here it is internalized and de-

graded via the lysosomes with a half-time of 4–6 h (Caughey et al., 1989; Borchelt et al., 1990).

In this study, we examined the effects of FK506 treatment on the biogenesis of PrP^C. We show that in drug-treated cells, the expression of PrP^C is selectively reduced in a process that does not depend on calcineurin inhibition or degradation via lysosomes. Instead, FK506 increases abortive translocation of PrP^C and subsequent proteasomal degradation. Furthermore, in mouse cells, knockdown of one of the six ER luminal FKBPs, FKBP10, induces PrP degradation almost as potently as FK506 treatment, although this occurs at a stage after translocation and involves both lysosomal and proteasomal pathways. Both FK506 treatment and FKBP10 depletion effectively inhibit propagation of PrP^{Sc} in a mouse neuroblastoma cell model.

RESULTS

FK506 treatment down-regulates PrP^C expression

The mouse neuroblastoma N2a cell line was used to assess the effect of FKBP inactivation on endogenous PrP^C expression. Under control conditions, an immunoblot of PrP^C revealed three isoforms that differed in extent of Asn-linked glycosylation from zero to two glycans (Figure 1A; Orsi et al., 2007). In addition, a minor proteolytic C1 cleavage product could be detected at ~20 kDa in some experiments (e.g., see ## in Figure 2; Liang et al., 2012). After overnight treatment with 20 μg/ml FK506, PrP^C levels were found to be substantially reduced compared with the ER-resident Hsp70 protein BiP or cytosolic glyceraldehyde-3-phosphate dehydrogenase (GAPDH; Figure 1A). This selective down-regulation of PrP was also observed by flow cytometry, increasing in magnitude as a function of FK506 concentration over the range 0–20 μg/ml (Figure 1B). In contrast, surface major histocompatibility complex (MHC) class I expression was unaffected by drug treatment. Cell viability was not affected over this concentration range, nor was there an induction of the unfolded protein response (UPR), as evidenced by lack of increased BiP expression (Figure 1A) and absence of spliced Xbp1 transcription factor mRNA (Figure 1C). The lack of a detectable UPR is important because this stress response was previously shown to be associated with a preemptive quality control mechanism resulting in reduced PrP^C translocation into the ER and its subsequent degradation by the proteasome (Kang et al., 2006).

We further evaluated whether the FK506-induced reduction in PrP^C expression was reproducible in a human cell line that expresses PrP^C. We used HepG2 hepatoma cells and examined endogenous PrP^C expression after treatment with FK506 or cyclosporin A (CsA), another immunosuppressive drug that, like FK506, acts by inhibiting calcineurin. As shown in Figure 1D, overnight treatment with 25 μg/ml FK506 resulted in a substantial reduction in PrP^C expression, whereas no effect was observed on the levels of the secretory proteins transferrin and albumin, ER-residing proteins (BiP and PDI), or the cytosolic protein GAPDH. In contrast, CsA treatment had no effect on PrP^C expression, indicating that the reduced expression associated with FK506 treatment was not mediated by inactivation of calcineurin. We further tested whether FK506 might be inhibiting PrP^C translation. We assessed this by pulse radiolabeling transiently transfected HepG2 cells with [^{35}S]Met and immunoisolating newly synthesized PrP^C (Figure 1E). Translation was not affected, since comparable amounts of radiolabeled PrP^C were recovered in the absence or presence of FK506, although there was a marked increase in nonglycosylated PrP^C with FK506. This suggested that the effect of FK506 treatment occurs posttranslationally, possibly at the level of PrP^C translocation into the ER or at subsequent stages of folding, presumably through the inactivation of ER-residing FKBPs.
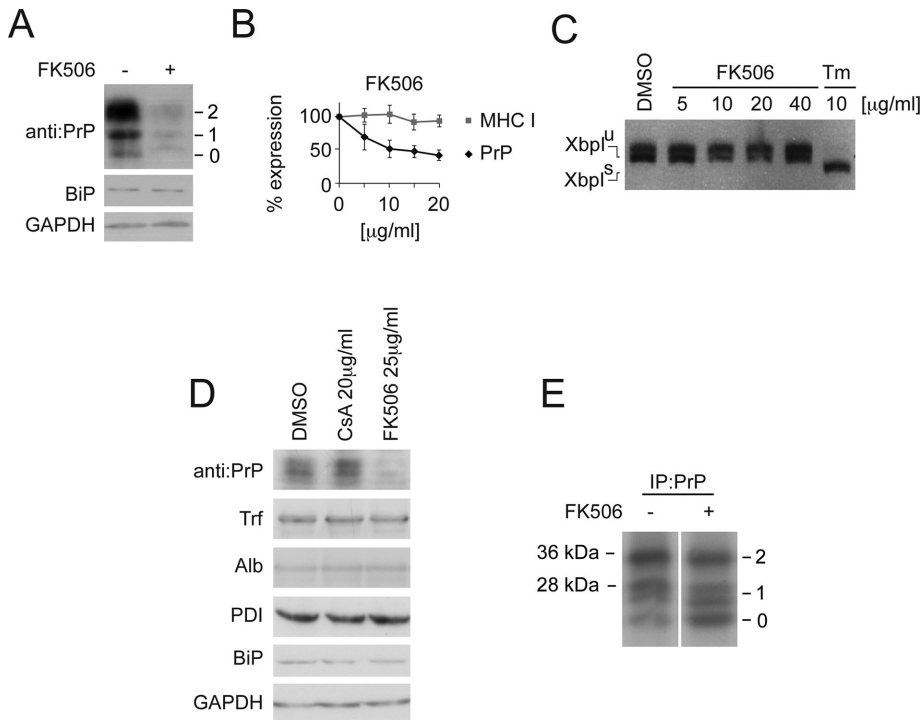
FIGURE 1: Effect of FK506 treatment on PrP^C expression. (A) N2a cells were treated with 20 µg/ml FK506 overnight, and the cell lysates were analyzed by immunoblotting for expression of endogenous PrP, BiP, and GAPDH. Here 0–2 indicate the different glycoforms of PrP^C. (B) FK506 at the indicated concentrations was incubated overnight with N2a cells, and the expression of endogenous PrP^C and MHC I was assessed by flow cytometry ($n = 4$, ±SD). (C) UPR activation was assessed by an *Xbp*I mRNA splicing assay, using RNA isolated from N2a cells after overnight incubation with FK506. Tunicamycin (Tm) was used as a positive control, and DMSO served as a vehicle control. (D) HepG2 cells were incubated with 20 µg/ml CsA or 25 µg/ml FK506 overnight, followed by immunoblotting for PrP^C, transferrin (Trf), albumin (Alb), PDI, BiP, and GAPDH. (E) N2a cells transiently transfected with a plasmid encoding hamster PrP were treated with DMSO or 20 µg/ml FK506 for 1 h. The cells were then starved in Met-free medium for 15 min and then radiolabeled with 150 µCi/ml [^{35}S]Met for 20 min in the continued presence of the drug. PrP^C was immunoisolated with mAb 3F4 and analyzed by SDS–PAGE and fluorography. Band doublets are due to the presence of both precursor and GPI-anchored forms of PrP^C (Orsi *et al.*, 2007).

FK506 treatment induces proteasome-mediated degradation of PrP^C

To further characterize the FK506-induced down-regulation of PrP^C expression, we examined the kinetics of the process. Figure 2, A and B, shows that total PrP^C expression, which mainly consists of cell surface PrP^C, dropped with a half-time of ~8 h during drug treatment. This is only slightly slower than the published turnover rates of surface PrP^C (4–6 h; Caughey *et al.*, 1989; Borchelt *et al.*, 1990), suggesting that relatively little newly synthesized PrP^C was reaching the plasma membrane to replenish the surface PrP^C pool. This was confirmed by repeating the time course after first removing cell surface PrP^C by a brief digestion with trypsin and then allowing cells to recover in the absence or presence of FK506 (Figure 2, C and D). Whereas control cells recovered steady-state PrP^C expression after ~10 h, the recovery of PrP^C expression was profoundly inhibited by FK506. Surprisingly, we also noted that after trypsin treatment, the PrP^C that reached the cell surface after overnight recovery in the absence or presence of FK506 treatment differed in its sensitivity to phospholipase C (PI-PLC) digestion (Supplemental Figure S1). Whereas cell surface PrP^C in control cells exhibited the expected sensitivity to PI-PLC, reflecting its GPI anchorage, the small portion of PrP^C that reached the cell surface in FK506-treated cells was

largely resistant to digestion, consistent with the loss of its GPI anchor. This was observed by flow cytometry (Supplemental Figure S1A) and immunoblotting (Supplemental Figure S1C). Control experiments revealed that sensitivity to trypsin digestion remained unaltered and that transmembrane-anchored MHC class I molecules were unaffected by either PI-PLC or trypsin treatment (Supplemental Figure S1B).

Because PrP^C translation was normal in FK506-treated cells (Figure 1E), it seemed likely that its impaired expression was due to degradation at some stage after translation. Repeating the experiment of Figure 2C in the presence of bortezomib, a potent inhibitor of proteasome activity, confirmed this notion. Under these conditions (Figure 2E), PrP^C expression could be largely rescued after trypsin treatment. Strikingly, the predominant species of PrP^C that accumulated in FK506- and bortezomib-treated cells migrated more rapidly than the PrP^C within cells lacking FK506 (Figure 2E), being similar to a nonglycosylated form of PrP^C (see Figure 4 later in this article). This species appeared to be present at low levels in FK506-treated cells in the absence of proteasome inhibitor as in Figure 2C, but its presence was highly variable and in many cases undetectable (e.g., Figures 2A and 1D). It has also been reported that FK506 treatment induces autophagy and that autolysosomal activity is responsible for the drug-induced enhancement of PrP^{Sc} degradation observed in prion-infected cells (Nakagaki *et al.*, 2013). To test whether lysosomal degradation contributes to the observed reduction of PrP^C expression in FK506-treated cells, we compared the abilities of chloroquine and lactacystin, inhibitors of lysosomal and proteasomal degradation, respectively, to inhibit PrP^C degradation. As shown in Figure 3A, lactacystin treatment clearly inhibited PrP^C degradation in the presence of FK506, whereas chloroquine had little, if any, effect. In the absence of FK506, chloroquine increased all forms of PrP^C, as expected, given the normal turnover of PrP^C in lysosomes.

FK506 down-regulates PrP^C expression by potentiating abortive translocation into the ER

There are several stages in PrP^C proteostasis at which FK506 could potentially induce proteasomal degradation, such as abortive translocation of PrP^C into the ER or ER-associated degradation (ERAD) of misfolded PrP^C after its translocation. It is also conceivable that newly synthesized PrP^C could reach the cell surface but is rapidly internalized and degraded. To test the latter possibility, we incubated control and drug-treated N2a cells in the presence of 0.025% trypsin overnight to continuously remove any PrP^C appearing on the surface of the cells. As shown in Figure 3B (lanes 4 and 8), trypsin treatment had little effect on the accumulation of PrP^C associated with FK506 and lactacystin treatment, strongly suggesting that the PrP^C destined for degradation did not pass through the cell surface.
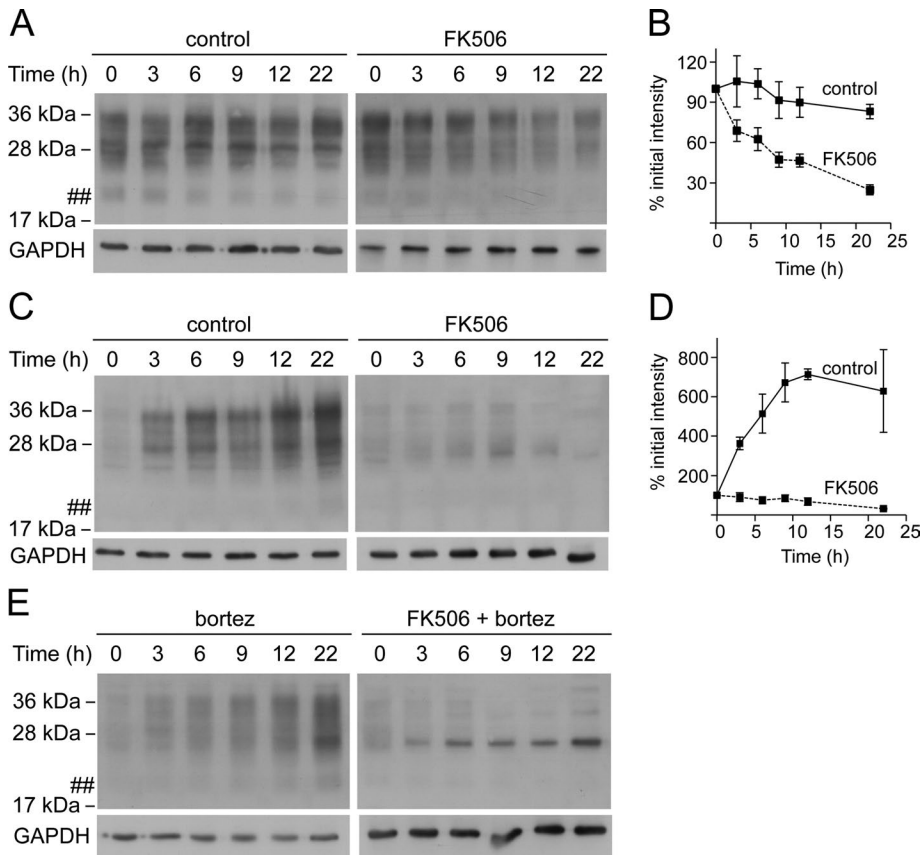
FIGURE 2: FK506 treatment induces proteasome-mediated degradation of PrP^C. (A) N2a cells were incubated with DMSO or 20 µg/ml FK506 for the indicated times, and PrP^C expression was monitored by immunoblotting. (B) PrP^C bands in A were quantified by densitometry, normalized to the GAPDH loading control, and expressed as a percentage of the protein present at the 0-min time point ($n = 6$, ±SEM). (C) N2a cells were digested with trypsin to remove surface PrP^C and then treated with DMSO or 20 µg/ml FK506 for periods up to 22 h. The recovery of PrP^C expression was monitored by immunoblotting. (D) Quantitation ($n = 6–7$, ±SEM). (E) The experiment in C was repeated with the addition of 5 µM bortezomib (bortez) to inhibit proteasome activity.

To test whether FK506 was inducing ERAD of PrP^C, we knocked down components of the ERAD machinery and assessed whether this affected the drug-induced degradation of PrP. We used human U373-MG cells, due to their high efficiency of infection with the lentivirus used for short interfering RNA (shRNA) knockdowns. Two

ERAD components were chosen for knockdown: SEL1L, a binding partner of the Hrd1 E3 ubiquitin ligase that is involved in ERAD of many misfolded soluble and some membrane proteins (Sun *et al.*, 2014), and VCP, an AAA-ATPase that plays a central role in ERAD of most misfolded substrates regardless of their topology (Lilley *et al.*, 2004; Ye *et al.*, 2004). Control and knockdown cells were treated with 20 µg/ml FK506 overnight, and surface PrP^C expression was measured using flow cytometry (Supplemental Figure S2A). Neither of the knockdowns had any effect on the FK506-induced reduction in PrP^C expression despite their effectiveness in inhibiting the ERAD of MHC class I molecules induced by the human cytomegalovirus immunoevasin protein US11 (Supplemental Figure S2B). These findings suggest that ERAD was an unlikely mechanism for the degradation of PrP^C during FK506 treatment.

We next assessed the possibility that FK506 enhances abortive translocation of nascent PrP. It is well established that PrP^C possesses an inefficient signal sequence that results in as much as 20% of the protein failing to translocate into the ER and subsequently undergoing degradation by the proteasome (Rane *et al.*, 2004). This abortive translocation can be reduced by replacing the PrP^C signal sequence with those of proteins that are more efficiently translocated (Rane *et al.*, 2004). For these experiments, mouse N2a cells were transiently transfected with plasmids encoding hamster PrP^C preceded either by its own signal sequence or the signal sequences of the more efficiently translocated proteins osteopontin (Opn) and prolactin (Prl). After 24 h, the transfectants were treated with or without FK506 overnight, and hamster PrP^C expression was evaluated by immunoblotting with monoclonal antibody (mAb) 3F4. Similar to endogenous PrP^C, FK506 treatment induced the degradation of hamster PrP^C containing its natural signal sequence (Figure 4A, lane 2), and this could be blocked by inhibiting proteasome activity, with concomitant accumulation of a rapidly migrating form of PrP^C (Figure 4A, lane 3, arrowhead). In marked contrast, FK506 had no effect on the expression of PrP^C containing the osteopontin or prolactin signal sequences. Similarly, proteasome inhibition did not cause the accumulation of the rapidly migrating species observed in the case of wild-type hamster PrP^C, although some variable increases in nonglycosylated PrP^C were seen for all three constructs (Figure 4A, lanes 3, 6, and 9, denoted as 0). Because the degradation of PrP^C induced by FK506 treatment can be bypassed by replacing the PrP^C signal sequence with more efficiently translocated
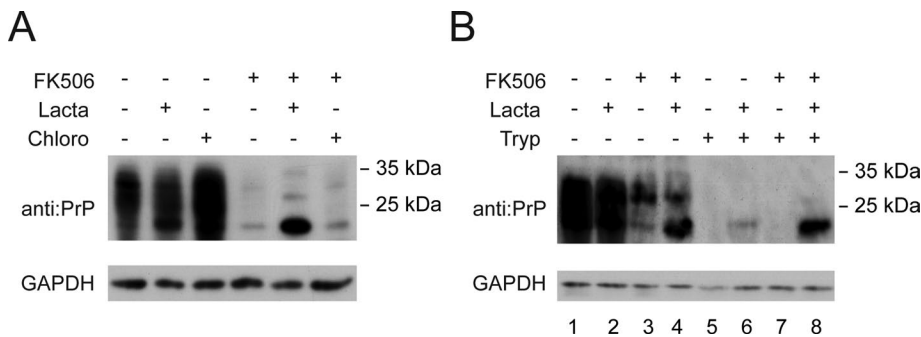

FIGURE 3: FK506 down-regulation of PrP^C is not mediated by internalization and lysosomal degradation. (A) N2a cells were treated with 20 µg/ml FK506 or DMSO in combination with 25 µM chloroquine (Chloro) or 25 µM lactacystin (Lacta) overnight. PrP^C expression was subsequently measured by immunoblotting. (B) N2a cells were incubated in serum-free DMEM with 20 µg/ml FK506 or DMSO in combination with 25 µM lactacystin and/or 0.025% trypsin (Tryp) overnight as indicated. PrP^C expression was then measured by immunoblotting.
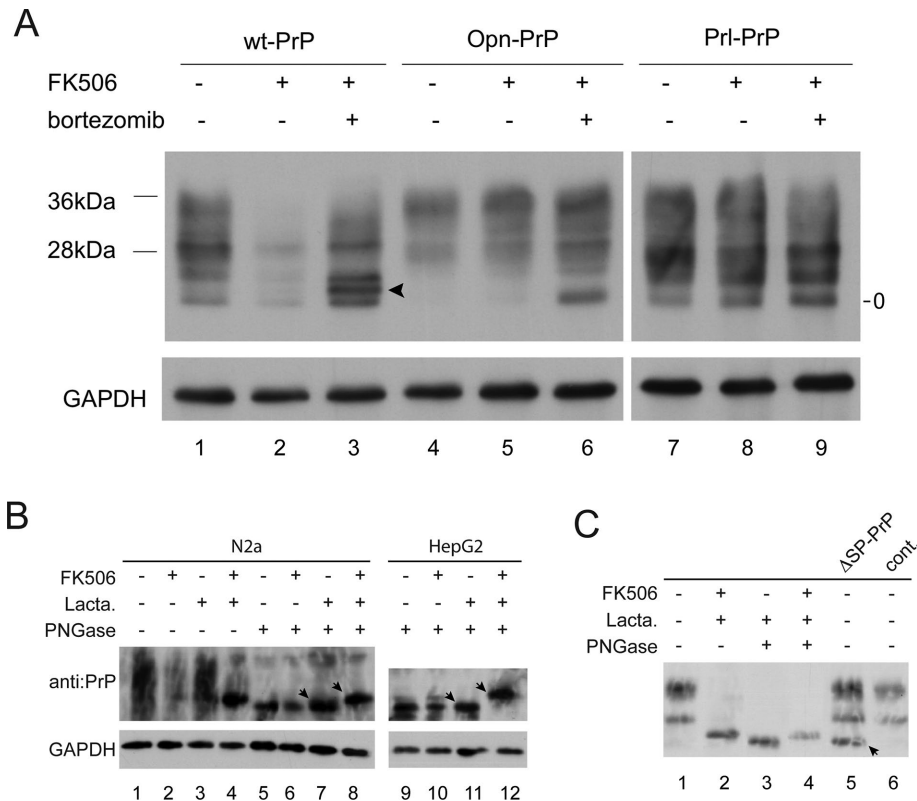
FIGURE 4: FK506 treatment enhances abortive translocation of PrP^C. (A) N2a cells were transiently transfected with plasmids encoding hamster PrP^C with either its wild-type (wt) signal sequence or that of osteopontin (Opn) or prolactin (Prl). After overnight treatment with DMSO or 20 µg/ml FK506 in the absence or presence of 5 µM bortezomib, cell lysates were immunoblotted with mAb 3F4 to selectively detect hamster PrP^C. (B) N2a or HepG2 cells were treated overnight with DMSO, or 20 or 25 µg/ml FK506, respectively, in the absence or presence of 25 µM lactacystin. Cell lysates were split and digested with or without PNGase as indicated, followed by immunoblotting to detect PrP^C. Arrows indicate the reduced mobility of PrP^C that accumulates in FK506- and lactacystin-treated cells. (C) N2a cells were treated overnight with DMSO or 20 µg/ml FK506 in the absence or presence of 25 µM lactacystin as indicated. Cell lysates were split and subjected to PNGase digestion or left untreated. These samples were compared with N2a cells transiently transfected with control plasmid or plasmid encoding mouse ΔSP-PrP^C, which lacks a signal sequence. The mobility of ΔSP-PrP^C is indicated by the arrow. In all of these experiments, the SDS–PAGE gels were run for extended times to increase the resolution between the unglycosylated signal-cleaved and signal-uncleaved species. These forms of PrP^C were typically not resolved under the SDS–PAGE conditions of the preceding figures.

signals, the results demonstrate that FK506 is indeed enhancing the abortive translocation of PrP^C.

PrP^C that fails to translocate into the ER would be expected to lack Asn-linked oligosaccharides and retain its signal sequence. Consequently, we examined the mobility of PrP^C that accumulates upon inhibiting proteasomal degradation in FK506-treated cells. This species was found to be nonglycosylated based on its resistance to digestion with peptide N-glycanase F (PNGase; Figure 4B, compare lanes 4 and 8). Furthermore, it had a distinctly slower mobility than signal-cleaved, deglycosylated, and GPI-anchored PrP^C from control cells (compare lanes 7 and 8 in N2a cells and lanes 11 and 12 in HepG2 cells; arrows). This mobility difference could arise either at the N-terminus due to differences in signal peptide cleavage or at the C-terminus as PrP^C undergoes conversion from a transmembrane form to a GPI-anchored form. To test the influence of GPI anchorage on electrophoretic mobility, we compared signal-cleaved, deglycosylated, and GPI-anchored PrP from control cells

with transiently expressed ΔSP-PrP^C that lacks a signal sequence and hence is directed to the cytosol where it retains its C-terminal transmembrane (TM) segment. The latter construct was expressed in the presence of endogenous PrP^C but is well resolved as the most rapidly migrating species (Figure 4C, lane 5, arrow). As shown in Figure 4C, no difference was observed in the mobilities of signal-cleaved, deglycosylated, and GPI-anchored PrP^C (lane 3) and ΔSP-PrP^C (lane 5), indicating little influence of TM cleavage and GPI anchorage on electrophoretic mobility in our system. Of importance, the species accumulating after FK506 and lactacystin treatment (Figure 4C, lanes 2 and 4) migrated more slowly than either of the signal-cleaved TM-anchored (Figure 4C, lane 5) or GPI-anchored species (Figure 4C, lane 3), consistent with the accumulated PrP^C having an intact N-terminal signal sequence, as would be expected if it fails to translocate into the ER.

Depletion of ER-localized FKBP10 down-regulates PrP^C expression

The observed effects of FK506 were presumably due to its inhibition of one or more FK-BPs involved in supporting the translocation of PrP^C into the ER. As a first step to identifying the FKBPs involved, we assessed the steady-state mRNA levels of all cytosolic and ER luminal FKBPs in human HepG2 cells. As shown in Supplemental Figure S3A, the most abundant mRNAs were those encoding cytosolic FKBP1A (also known as FKBP12) and ER-localized FKBP10 (FKBP65), which made them attractive candidates for involvement in PrP^C translocation. RNA interference was then used to deplete all 12 FKBPs individually to assess their effects on PrP^C expression. Knockdown efficiency ranged from 70 to 95% (Supplemental Figure S3B), but surprisingly little effect was observed on PrP^C expression (Supplemental Figure S3C). Only in the case of FKBP10 depletion was a substantial reduction in PrP^C expression observed in several of the replicates (40–60% reduction in four of 18 replicates). The failure to recapitulate the effects of FK506 treatment by depleting individual FKBPs suggested that there might be some functional overlap between family members.

The attenuation of PrP^C expression that was observed in a few cases of FKBP10 depletion was intriguing, and we decided to pursue this further in mouse N2a cells. In contrast to humans (Barnes et al., 2012), mice with an FKBP10-null mutation do not survive birth, suggesting that there might be less functional overlap between family members within this species (Lietman et al., 2014). Consistent with this view, depletion of FKBP10 by RNA interference in N2a cells reduced PrP^C expression almost as effectively as FK506 treatment (Figure 5A and Supplemental Figure S4). Again, this effect was selective, in that other proteins, such as the ER Hsp70 chaperone BiP, cytosolic GAPDH, and the GPI-anchored cell surface protein CD90, exhibited no reduction in expression.
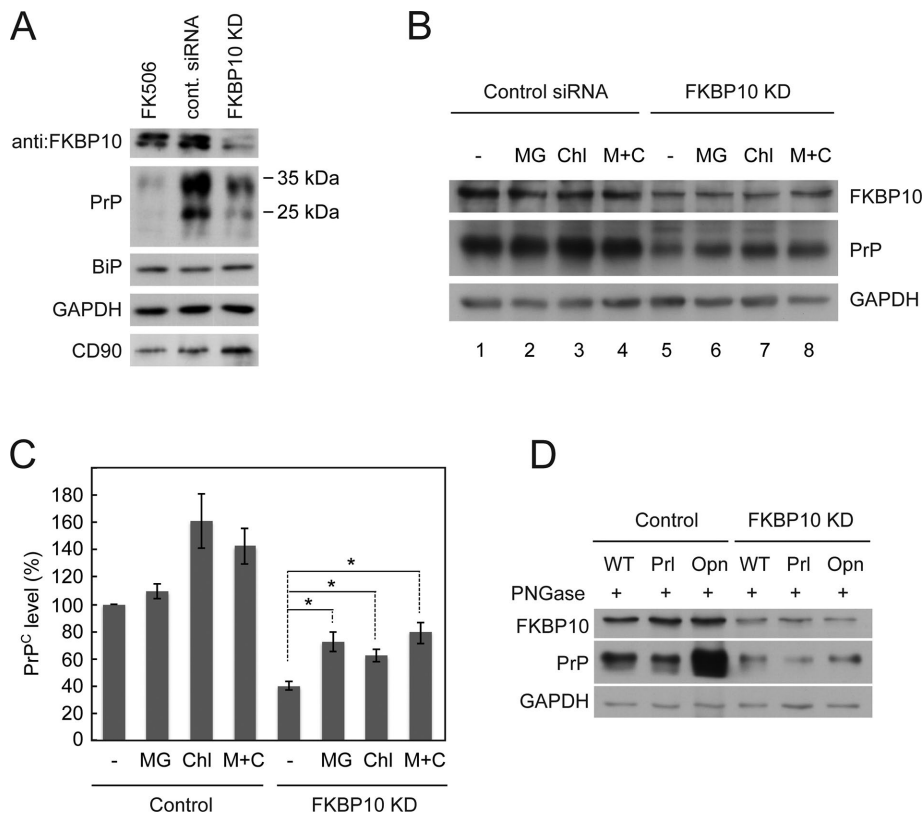
FIGURE 5: FKBP10 depletion induces degradation of PrP[C] through proteasomal and lysosomal pathways. (A) Knockdowns (KDs) were performed over a period of 7 d in N2a cells using either FKBP10-specific siRNA or nontargeting control siRNA, and FKBP10 expression was assessed by immunoblot. Expression levels of PrP[C], BiP, GAPDH, and CD90 were also monitored. For comparison, N2a cells were treated with 25 µg/ml FK506 overnight. (B) N2a cells were treated with FKBP10-specific siRNA or control siRNA for 3 d and subsequently treated with DMSO, 10 µM MG132 (MG), 25 µM chloroquine (Chl), or both (M+C) for 16 h. After deglycosylation with PNGase, FKBP10, PrP[C] and GAPDH levels were assessed by immunoblot. (C) Densitometric quantification of PrP[C] levels was carried out using ImageJ software (National Institutes of Health, Bethesda, MD). Values are expressed as a percentage of the level in control siRNA + vehicle–treated cells ($n = 4$ for FKBP10 siRNA + M+ C; $n = 5$ for all other conditions, ±SEM). *$p < 0.005$. (D) Knockdowns were performed over a period of 6 d in N2a cells using either FKBP10-specific siRNA or nontargeting control siRNA. In addition, the cells were transiently transfected on day 5 with plasmids encoding hamster PrP[C] with either its WT signal sequence or that of Prl or Opn. After deglycosylation with PNGase, the expression levels of FKBP10, PrP[C], and GAPDH were monitored by immunoblot.

Because FKBP10 knockdown results in down-regulation of PrP[C] in a manner similar to FK506 treatment, it was important to test whether it also occurs by enhancing abortive translocation. We first assessed whether the loss of PrP[C] could be blocked by inhibiting proteasome or lysosome activity. To facilitate quantitation of the effects of inhibitors, samples were deglycosylated with PNGase F. We were surprised to note that the addition of the proteasome inhibitor MG132 only partially blocked degradation and that the addition of chloroquine also partially blocked degradation, indicating that the loss of PrP[C] was occurring by both proteasomal and lysosomal processes (Figure 5B, compare lanes 5–7; quantified in Figure 5C). This was supported by immunofluorescence microscopy, which revealed the accumulation of PrP[C] in LAMP1-positive structures upon FKBP10 depletion in the absence or presence of chloroquine, as well as its accumulation in nonlysosomal compartments upon MG132 treatment (Supplemental Figure S5). Furthermore, the mobility of deglycosylated PrP[C] accumulating upon FKBP10 knockdown and either MG132 or chloroquine treatment was similar to that of deglycosyl-

ated PrP[C] in control cells, suggesting that its signal sequence had been cleaved (Figure 5B). We then expressed the PrP[C] variants possessing prolactin and osteopontin signal sequences in FKBP10-depleted cells. These more efficiently translocated variants were degraded to a similar extent as wild-type PrP[C] in FKBP10-depleted cells (Figure 5D). Collectively these results indicate that, in contrast to FK506 treatment, FKBP10 depletion does not enhance the abortive translocation of PrP[C]. Instead, the data are consistent with translocation of PrP[C] into the ER, where it undergoes signal cleavage, glycosylation, and then disposal by both proteasomal and lysosomal degradation. The different phenotypes observed between FK506-treated and FKBP10-depleted cells suggest the contribution of additional FKBP family members that act upstream of FKBP10 during the biogenesis of PrP[C].

FK506 treatment or FKBP10 depletion impairs the propagation of scrapie PrP

Because FK506 or FKBP10 knockdown affected PrP[C] expression, we were interested in evaluating these approaches as a means to reduce the propagation of PrP[Sc]. Mouse scrapie-infected N2a (ScN2a) and scrapie mouse brain (SMB) cells that are chronically infected with scrapie prions and produce PrP[Sc] were treated for 6 d with different concentrations of FK506. The cells were subsequently lysed, and the cell lysates were split either for direct assessment of total PrP expression or for proteinase K (PK) digestion to monitor the levels of PK-resistant PrP[Sc]. As shown in Figure 6, FK506 not only reduced total PrP, but it also strongly inhibited the steady-state level of PK-resistant PrP[Sc] in both cell lines. Similarly, we evaluated the effect of FKBP10 depletion on PrP[Sc] propagation in the same cells. The knockdown efficiency was >90% for ScN2a cells and >70%

for SMB cells (Figure 7, A and B). Although the depletion of FKBP10 resulted in a rather modest reduction of total PrP expression (~40%), it nevertheless strongly depressed the level of PK-resistant PrP[Sc] by as much as 80% (Figure 7, A–D). This suggests that FKBP10 might constitute a novel target for the treatment of prion disease.

DISCUSSION

For susceptibility to infectious prions and the development of persistent prion disease, PrP[C] has to be expressed (Bueler et al., 1993; Brandner et al., 1996; Mallucci et al., 2003; Chesebro et al., 2005), which involves not only its translation, but also its subsequent translocation into the ER, GPI-anchoring, and export to the cell surface (Priola et al., 2009). The current understanding of the disease suggests that altering at least one of the foregoing processes may break the chain of events, leading to PrP[Sc] propagation and the development of disease (Mays et al., 2014). Several research groups reported a new potential therapeutic, FK506, which might be clinically useful against prion diseases (Mukherjee et al., 2010;
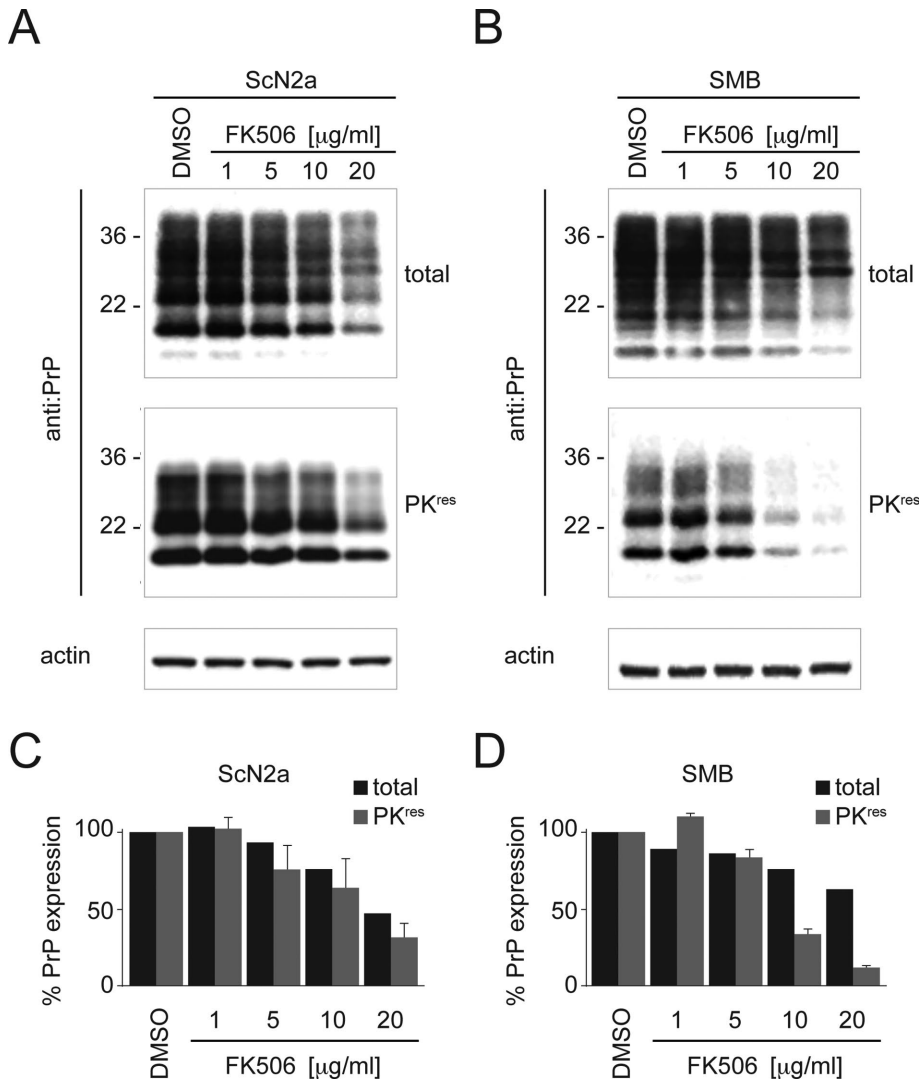
FIGURE 6: FK506 treatment effectively reduces PrP^{Sc} propagation. (A) ScN2a and (B) SMB cells were treated with DMSO or the indicated concentrations of FK506 for 6 d. The cells were lysed and split for the direct assessment of total PrP levels or for PK digestion and assessment of PK-resistant PrP^{Sc} levels. Total PrP and PrP^{Sc} were quantified and expressed as a percentage of the level in DMSO-treated control cells for (C) ScN2a and (D) SMB cell lines ($n = 3$, ±SD).

cytosolic, ER-resident, and cell surface proteins, including another GPI-anchored protein, CD90. Furthermore, drug treatment did not induce an ER unfolded protein response. It was crucial to control for UPR because a similar phenotype of enhanced abortive translocation of PrP has been reported in response to dithiothreitol (DTT)- or thapsigargin-induced stress, which might serve as a means to minimize the toxicity associated with PrP^C misfolding within the ER (Kang et al., 2006). The observed effects of FK506 were not mediated by calcineurin inhibition, as previously suggested (Mukherjee et al., 2010), since a second inhibitor of calcineurin, cyclosporin A, had no effect on PrP^C expression. However, this does not exclude the possibility that FK506-mediated inhibition of calcineurin function might be an important additional contributor to the reduced neurotoxicity observed in PrP^{Sc}-infected cells and mice (Mukherjee et al., 2010). Similarly, neither we nor other workers could detect evidence of FK506-induced autophagic degradation of PrP^C (Karapetyan et al., 2013). This appears to contrast with a report that FK506 treatment activates autophagy to enhance PrP^{Sc} degradation in both cell and animal models of prion infection (Nakagaki et al., 2013). However, because it is well established that autophagy is a major pathway of PrP^{Sc} degradation (reviewed in Goold et al., 2015), the latter observation might be specific to aggregated PrP^{Sc} and raises the possibility that both PrP^C reduction through abortive translocation and the autophagic disposal of PrP^{Sc} both contribute to the reported improved pathology and prolonged survival of prion-infected mice treated with FK506 (Mukherjee et al., 2010; Nakagaki et al., 2013).

Karapetyan et al., 2013; Nakagaki et al., 2013). Its utility was variously ascribed to its inhibition of the elevated calcineurin activity observed in PrP^{Sc}-treated cells and mice (Mukherjee et al., 2010), a reduction in PrP^C expression at an undefined posttranscriptional stage (Karapetyan et al., 2013), or induction of autophagy to accelerate the degradation of PrP^{Sc} (Nakagaki et al., 2013). Here we show that FK506 effectively reduces PrP^C expression, and it does so by enhancing its abortive translocation and accompanying degradation by the proteasome. Furthermore, the residual PrP^C that reaches the cell surface suffers from inefficient GPI anchoring, which, together with reduced PrP^C expression, translates into profoundly reduced propagation of PrP^{Sc} in in vitro cell models. We also show that in mouse cells, depletion of a single ER family member, FKBP10, strongly down-regulates PrP^C expression and reduces cellular propagation of PrP^{Sc}. However, FKBP10 depletion affects PrP^C biogenesis at a later stage after translocation, resulting in its disposal by both proteasomal and lysosomal pathways.

The abortive translocation and degradation of PrP^C was specific, since FK506 treatment did not affect the levels of a variety of

How does FK506 potentiate the abortive translocation of PrP^C? It is well established that N-terminal signal sequences differ substantially in efficiency and that the signal sequence of PrP^C is measurably less efficient than other signal sequences, such as that of prolactin (Kang et al., 2006). This leads to the constitutive production of ~10–20% of PrP^C molecules that are not translocated into the ER and are degraded by the proteasome. An investigation into factors contributing to differences in translocation efficiency revealed that proteins with less efficient signals like PrP^C depend on trans-acting factors such as translocating chain-associating membrane protein (TRAM; Voigt et al., 1996), the translocon-associated protein complex (TRAP; Fons et al., 2003), and soluble ER luminal proteins (Kang et al., 2006), whereas proteins like prolactin can translocate efficiently in their absence. Indeed, just replacing the PrP^C signal sequence with that of preprolactin can bypass these requirements. One potential explanation for the effects of FK506 on PrP^C translocation is that it might induce changes in isomerization state of a proline residue within the PrP^C signal sequence, leading to even less efficient signal function. However, an examination of the mouse and
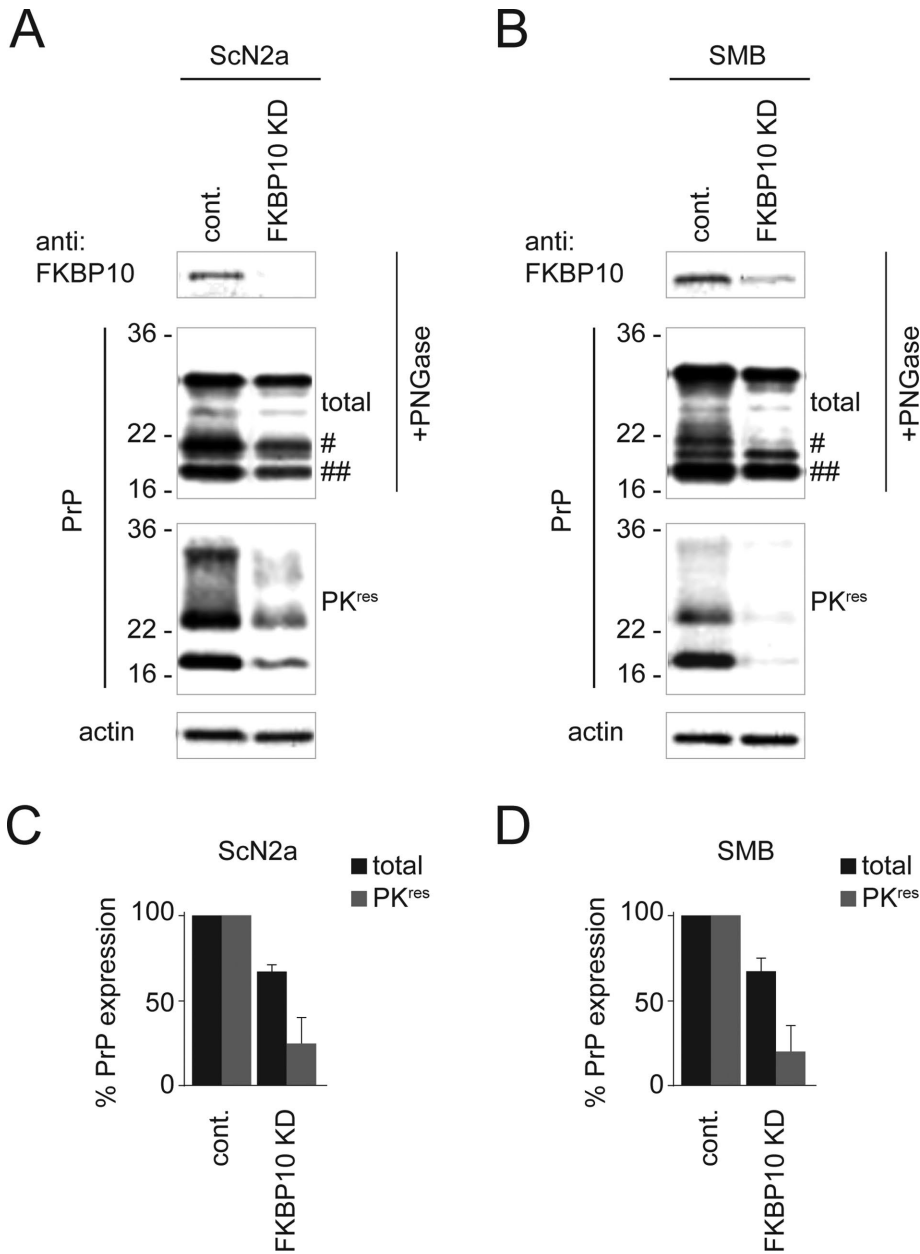
FIGURE 7: FKBP10 depletion effectively inhibits PrP^Sc propagation. FKBP10 knockdown was performed transiently using siRNA in (A) ScN2a and (B) SMB cells. The efficiencies of the knockdowns were validated in PNGase-treated lysates by immunoblotting for FKBP10 with actin as loading control. To evaluate PrP and PrP^Sc levels, cell lysates were split for the direct assessment of total PrP levels after PNGase treatment or for PK digestion and assessment of PK- resistant PrP^Sc. Here # and ## indicate C2 and C1 PrP fragments, respectively. Total PrP and PrP^Sc were quantified and expressed as a percentage of the level in control cells for (C) ScN2a and (D) SMB cell lines ($n = 4$, ±SD).

quences during translocation (High *et al.*, 1993), or TRAP, a multispan membrane complex of four subunits (Hartmann *et al.*, 1993), enhances translocation in a signal-sequence dependent manner remains unclear. However, alterations in proline isomerization state in either protein might modulate function sufficiently to affect the translocation of those proteins with the least efficient signal sequences such as PrP^C. Alternatively, given that undefined ER luminal proteins also affect translocation efficiency in a signal sequence–dependent manner (Kang *et al.*, 2006), there are potentially additional candidates whose functions could be modulated by loss of FKBP activity.

In an effort to identify FKBPs whose functions contribute to the translocation of PrP^C, we individually depleted 12 FKBP family members within the ER and cytosol of human HepG2 cells. Unfortunately, none of the single knockdowns could recapitulate the reduced PrP^C expression observed with FK506 treatment, which suggested the possibility of functional overlap between FKBP family members. In contrast to human HepG2 cells, we found that in mouse N2a cells, individual depletion of ER luminal FKBP10 was associated with a profound reduction in PrP^C expression. This might be due to less functional overlap between ER luminal FKBPs in mouse cells compared with human cells. Indeed, recent work showed that the FKBP10-null phenotype is more severe in mice, since they do not survive birth, whereas in humans, the deficiency is associated with osteogenesis imperfecta (Barnes *et al.*, 2012; Lietman *et al.*, 2014). Surprisingly, the mechanism of PrP^C down-regulation in FKBP10-depleted mouse cells differed from the abortive translocation observed in cells treated with FK506. On FKBP10 depletion, PrP^C underwent signal cleavage and was degraded by both proteasomal and lysosomal processes. Furthermore, replacement of the PrP^C signal sequence with more efficiently translocated signal sequences failed to bypass this degradation. Collectively these findings suggest that FKBP10 is acting after translocation, most likely during PrP^C folding, and that its depletion results in PrP^C disposal both by

human PrP^C signal sequences reveals no candidate proline residues that could be affected in this manner. Alternatively, *trans*-acting factors like TRAM and TRAP are candidates for proteins whose functions might be affected by FK506 treatment. Because FK506 binds to the active sites of all cellular FKBPs and inhibits their activities, it appears that it is the impaired peptidyl prolyl isomerase function of one or more FKBPs that underlies this translocation arrest rather than the involvement of an associated chaperone function that has been reported for several of the family members (Barik, 2006). How TRAM, a multispanning membrane protein that contacts signal se-

ERAD and after export to lysosomes. Of interest, this function of FKBP10 does not appear to require its peptidyl prolyl isomerase activity, since efficiently translocated variants of PrP^C (possessing signal sequences from preprolatin and osteopontin) were not subjected to degradation when all FKBP activities (including FKBP10) were inhibited by FK506 treatment (Figure 4A). This is consistent with previous reports indicating that FKBP10 can act as a chaperone, independently of its enzymatic activity, to delay in vitro fibril formation of type I collagen (Ishikawa *et al.*, 2008) and assembly of tropoelastin fibrils (Cheung *et al.*, 2010; Miao *et al.*, 2013), as well as to

enhance the degradation of mutant glucocerebrosidase by ERAD (Ong *et al.*, 2013). The distinct differences in PrP^C phenotypes between FK506 treatment, which causes abortive translocation, and FKBP10 depletion, which affects PrP^C posttranslocation, suggests that FKBP family members act at distinctly different stages in PrP^C biogenesis. Efforts are ongoing in various cell lines to identify those members acting upstream of FKBP10 that enhance the efficiency of PrP^C translocation.

We tested both FK506 treatment and FKBP10 knockdown for their effectiveness in reducing PrP^{Sc} propagation in cell models. In both cases, the approaches were found to reduce PrP^{Sc} levels by 75–90%, suggesting that either strategy might be of therapeutic value. Of interest, FK506 was tested in animal models of prion disease before and was shown to be successful in extending survival in two of three studies (Mukherjee *et al.*, 2010; Karapetyan *et al.*, 2013; Nakagaki *et al.*, 2013). In each case, FK506 treatment was initiated well after the initial infection, 20 d later for intracerebral inoculation and 210 d later for intraperitoneal administration. With our insight into the effects of FK506 treatment on down-regulating PrP^C expression and its potency in reducing PrP^{Sc} propagation in cell-based systems, future animal studies could be designed with FK506 treatment starting before or soon after the infection with PrP^{Sc}. The complicating effects of immunosuppression might be mitigated through the use of analogues that retain FKBP binding but exhibit less immunosuppressive activity (Xiao *et al.*, 2007). Furthermore, our study identifies FKBP10 as a potential new therapeutic target for the treatment of prion disease that may have particular applicability to nonhuman species, in which there might be less functional overlap between FKBP family members. Species of interest include wild deer, elk, and other ruminants in which chronic wasting disease is prevalent. The identification of an inhibitor selective for FKBP10 is an exciting avenue for future investigation.

MATERIALS AND METHODS
Cell culture
Mouse neuroblastoma N2a cells, human hepatoma HepG2 cells, and human glioblastoma astrocytoma U373-MG cells were cultured in high-glucose DMEM (Life Technologies, Burlington, Canada) supplemented with 100 IU/ml penicillin, 100 µg/ml streptomycin, 2 mM L-glutamine, and 10% fetal bovine serum (FBS). ScN2a (Butler *et al.*, 1988) and SMB (Clarke *et al.*, 1970) cells were cultured in high-glucose DMEM (Life Technologies) supplemented with 10% FBS.

Antibodies and plasmids
The following antibodies were used: anti-BiP (BD Biosciences, Mississauga, Canada), anti-albumin, anti-transferrin, and anti-mouse actin (Sigma-Aldrich), anti-GAPDH (mAb 6C5; Millipore, Toronto, Canada), anti-human or hamster PrP (mAb 3F4; Cedarlane, Burlington, Canada), anti-mouse PrP (mAb Sha31; Bertin Pharma, Montigny le Bretonneux, France), anti-human MHC I (mAb W6/32; Ziegler *et al.*, 1982), anti-mouse MHC I (mAb Y3; Jones *et al.*, 1981), anti-PDI (AssayDesigns, Farmingdale, NY), anti-CD90 (Abcam, Cambridge, MA), anti-mouse FKBP10 (BD Biosciences), anti-human FKBP10 (Abcam) and anti-mouse LAMP1 (mAb 1D4B; Developmental Studies Hybridoma Bank, University of Iowa, Iowa City, IA).

pcDNA3.1 plasmids encoding wild-type hamster PrP^C or hamster PrP^C with its N-terminal signal sequence replaced with that of rat osteopontin or bovine prolactin were obtained from R. Hegde (MRC Laboratory of Molecular Biology, Cambridge, United Kingdom). ΔSP-PrP that encodes mouse PrP lacking its N-terminal signal sequence was generated by PCR from full-length mouse PrP cDNA in pcDNA3.1 using the following primers: forward primer,

5′-ACGGGATCCATGAAAAAGCGGCCAAAGCCTGGAG; and reverse primer, 5′-CGAGCGGCCGCTCATCCCACGATCAGGAA-GATGA. The fragment was ligated into a new pcDNA3.1 plasmid using *Bam*HI and *Not*I restriction sites.

Plasmid transfection
Transfections were performed in six-well plates. pcDNA plasmids (1–4 µg) were mixed with 250 µl of OptiMEM (Life Technologies) and then combined with 12 µl of Lipofectamine 2000 previously diluted in 250 µl of OptiMEM. After 15 min, the mixture was added to plates of 50% confluent cells in 2 ml of DMEM without serum. After 4 h, the medium was adjusted to 10% with serum. The cells were grown for 24 h and then treated with drugs as indicated and analyzed.

RNA interference
Knockdowns in HepG2 cells using small interfering RNA (siRNA) were performed as previously described (Rutkevich *et al.*, 2010, 2012). Knockdowns in N2a cells were performed with 50 nM of Stealth Select siRNA (Life Technologies) and 7.5 µl of Lipofectamine RNAiMAX (Life Technologies) in 3 ml of DMEM without serum or antibiotics. After 4 h, the medium was adjusted to 10% serum in a total of 5 ml. Both cell lines were transfected on day 1 and again on day 4, followed by analysis on day 7. Controls were performed with nontargeting negative control Stealth Select siRNA.

Knockdowns using shRNA were performed with pLKO.1 plasmids obtained from the RNAi Consortium (www.broadinstitute.org/rnai/trc), using their protocol for lentiviral production. In brief, 293T cells growing in T25 filter cap flasks were used as packaging cells and transfected using FuGENE 6 with 100 ng of envelope plasmid VSV-G/pMD2.G, 900 ng of packaging plasmid pCMV-dR8.74psPAX2, and 1 µg of targeting pLKO.1 plasmid. The cells were cultured for ~18 h after transfection, followed by a medium replacement containing 30% FBS. Virus was collected after 48 h and added to U373-MG cells in growth medium with 8 µg/ml Polybrene. Puromycin selection (1 µg/ml) was initiated 48 h postinfection for 3 d.

Quantitative PCR
The levels of various FKBP transcripts were analyzed under both steady-state and specific knockdown conditions. Untransfected HepG2 cells or cells that had been transfected with an FKBP-specific siRNA or a nontargeting negative control were subjected to total RNA extraction using the RNeasy Mini Kit (Qiagen, Toronto, Canada) and used in a reverse transcription experiment using the SuperScript VILO cDNA Synthesis Kit (Life Technologies). The resulting cDNA library was used to selectively amplify by real-time quantitative PCR FKBP transcripts using the Life Technologies TaqMan Gene Expression Master Mix on an Applied Biosystems 7500 Standard thermocycler. The primers and probes used were as follows: FKBP1A, Hs00356621_g1; FKBP1B, Hs00997682_m1; FKBP2, Hs00234404_m1; FKBP4, Hs00427038_g1; FKBP5, Hs01561006_m1; FKBP7, Hs00535040_m1; FKBP8, Hs01014664_m1; FKBP9, Hs01119941_m1; FKBP10, Hs00222557_m1; FKBP11, Hs01042990_g1; FKBP14, Hs00215735_m1; FKBP15, Hs00293374_m1; and β-actin, Hs01060665_g1. The relative levels of each FKBP transcript were normalized to that of the reference transcript, β-actin, using the delta delta threshold cycle (ΔΔC_t) method. Briefly, ΔΔC_t = [C_t(target, untreated) − C_t(reference, untreated)] − [C_t(target, treated) − C_t(reference, treated)]. The ratio of the target transcript to the reference transcript is equivalent to $2^{-\Delta\Delta Ct}$.

Analysis of PrP^C expression
N2a or HepG2 cells were treated overnight with either dimethyl sulfoxide (DMSO) or various concentrations of FK506 and then

analyzed for total PrP levels by immunoblotting or for surface PrP by flow cytometry. For time courses of PrP^C expression after DMSO or 25 µM FK506 treatment, cells were plated after trypsinization and allowed to recover for 24 h before drug addition. To monitor the kinetics of PrP^C recovery after surface removal by trypsinization, cells were plated and treated with DMSO or 25 µM FK506 immediately after being trypsinized. At each time point, cells were harvested by scraping and lysed in 1% SDS and 100 mM Tris, pH 8, boiled for 7 min, and vortexed vigorously. The lysates were cleared by centrifugation and the protein content of the supernatant determined by bicinchoninic acid assay (ThermoFisher, Burlington, Canada). Samples subjected to a PNGase F digestion were treated overnight at 37°C with 200 U of enzyme. All samples were precipitated by incubation with five volumes of cold methanol for 2 h at –70°C before being centrifuged, dried, and solubilized by boiling for 10 min in SDS–PAGE sample buffer containing 5 mM DTT. Proteins were separated using 15% SDS–PAGE and transferred onto methanol-activated polyvinylidene fluoride membranes, and PrP^C was detected by immunoblotting using enhanced chemiluminescence. Quantitation of bands was conducted by scanning films and subsequent measurement of band intensity with Quantity One software (Bio-Rad, Mississauga, Canada).

For flow cytometry, control and drug-treated cells were analyzed for surface PrP^C or MHC I expression using specific primary antibody and secondary anti-mouse immunoglobulin G labeled with Alexa Fluor 647 dye. A FACSCalibur flow cytometer (BD Biosciences) was used to collect the data; 10,000 events for each sample. The data were analyzed using FlowJo software (Tree Star, Ashland, OR).

Unfolded protein response assessment

As described previously (Rutkevich et al., 2010), total RNA was isolated from cells using the RNeasy kit (Qiagen) and subjected to one-step reverse transcription PCR (Qiagen) using either human or mouse Xbp1 amplification primers: human, 5′-GGAGTTAAGACAGCGCTTGG-3′ and 5′-GAGATGTTCTGGAGGGGGTGA-3′; mouse, 5′-GGCCTTGTGGTTGAGAACCAGGAG-3′ and 5′-GAGTCTGATATCCTTTTGGGCATTC-3′. As a positive control, cells were incubated with 10 µg/ml tunicamycin overnight.

Evaluation of PrP^{Sc}

ScN2a or SMB cells were incubated for 6 d with the indicated concentration of FK506 and then lysed and evaluated for PrP^{Sc} using proteinase K digestion as described previously (Mays et al., 2012). In brief, 125 µg of cell lysate protein was digested with 100 µg/ml proteinase K for 1 h at 37°C and then inactivated with 1 mM phenylmethylsulfonyl fluoride and analyzed by immunoblotting using mAb Sha31. Total PrP^C expression was evaluated by immunoblotting 50 µg of cell lysate protein.

Immunofluorescence microscopy

N2a cells were grown on acid-treated glass coverslips in 60-mm dishes. On day 3 after siRNA transfection, cells were fixed for 15 min in 3% paraformaldehyde, washed three times, and then permeabilized in 0.1% Triton X-100 in phosphate-buffered saline (PBS) for 15 min. Coverslips were washed three times and then incubated in PBS containing 10% FBS and 0.02% sodium azide for 30 min. Incubations with anti-PrP or LAMP1 primary antibodies were carried out for 2 h, followed by three washes and then incubation with Alexa Fluor 647– or 488–conjugated secondary antibodies for 1 h. After an additional three washes, coverslips were mounted onto slides using DAPI Fluoromount-G (Southern Biotech, Birmingham, AL) and

imaged using a Zeiss AxioObserverZ1 inverted confocal microscope with a 63× objective.

REFERENCES

Barik S (2006). Immunophilins: for the love of proteins. Cell Mol Life Sci 63, 2889–2900.

Barnes AM, Cabral WA, Weis M, Makareeva E, Mertz EL, Leikin S, Eyre D, Trujillo C, Marini JC (2012). Absence of FKBP10 in recessive type XI osteogenesis imperfecta leads to diminished collagen cross-linking and reduced collagen deposition in extracellular matrix. Hum Mutat 33, 1589–1598.

Borchelt DR, Scott M, Taraboulos A, Stahl N, Prusiner SB (1990). Scrapie and cellular prion proteins differ in their kinetics of synthesis and topology in cultured cells. J Cell Biol 110, 743–752.

Brandner S, Isenmann S, Raeber A, Fischer M, Sailer A, Kobayashi Y, Marino S, Weissmann C, Aguzzi A (1996). Normal host prion protein necessary for scrapie-induced neurotoxicity. Nature 379, 339–343.

Bueler H, Aguzzi A, Sailer A, Greiner RA, Autenried P, Aguet M, Weissmann C (1993). Mice devoid of PrP are resistant to scrapie. Cell 73, 1339–1347.

Butler DA, Scott MR, Bockman JM, Borchelt DR, Taraboulos A, Hsiao KK, Kingsbury DT, Prusiner SB (1988). Scrapie-infected murine neuroblastoma cells produce protease-resistant prion proteins. J Virol 62, 1558–1564.

Caughey B, Race RE, Ernst D, Buchmeier MJ, Chesebro B (1989). Prion protein biosynthesis in scrapie-infected and uninfected neuroblastoma cells. J Virol 63, 175–181.

Chesebro B, Trifilo M, Race R, Meade-White K, Teng C, LaCasse R, Raymond L, Favara C, Baron G, Priola S, et al. (2005). Anchorless prion protein results in infectious amyloid disease without clinical scrapie. Science 308, 1435–1439.

Cheung KL, Bates M, Ananthanarayanan VS (2010). Effect of FKBP65, a putative elastin chaperone, on the coacervation of tropoelastin in vitro. Biochem Cell Biol 88, 917–925.

Clarke MC, Haig DA (1970). Evidence for the multiplication of scrapie agent in cell culture. Nature 225, 100–101.

Drisaldi B, Stewart RS, Adles C, Stewart LR, Quaglio E, Biasini E, Fioriti L, Chiesa R, Harris DA (2003). Mutant PrP is delayed in its exit from the endoplasmic reticulum, but neither wild-type nor mutant PrP undergoes retrotranslocation prior to proteasomal degradation. J Biol Chem 278, 21732–21743.

Flanagan WM, Corthesy B, Bram RJ, Crabtree GR (1991). Nuclear association of a T-cell transcription factor blocked by FK-506 and cyclosporin A. Nature 352, 803–807.

Fons RD, Bogert BA, Hegde RS (2003). Substrate-specific function of the translocon-associated protein complex during translocation across the ER membrane. J Cell Biol 160, 529–539.

Goold R, McKinnon C, Tabrizi SJ (2015). Prion degradation pathways: potential for therapeutic intervention. Mol Cell Neurosci 66, 12–20.

Hartmann E, Gorlich D, Kostka S, Otto A, Kraft R, Knespel S, Burger E, Rapoport TA, Prehn S (1993). A tetrameric complex of membrane proteins in the endoplasmic reticulum. Eur J Biochem 214, 375–381.

High S, Martoglio B, Gorlich D, Andersen SS, Ashford AJ, Giner A, Hartmann E, Prehn S, Rapoport TA, Dobberstein B, et al. (1993). Site-specific photocross-linking reveals that Sec61p and TRAM contact different regions of a membrane-inserted signal sequence. J Biol Chem 268, 26745–26751.

Ishikawa Y, Vranka J, Wirz J, Nagata K, Bachinger HP (2008). The rough endoplasmic reticulum-resident FK506-binding protein FKBP65 is a molecular chaperone that interacts with collagens. J Biol Chem 283, 31584–31590.

Jones B, Janeway CA Jr (1981). Cooperative interaction of B lymphocytes with antigen-specific helper T lymphocytes is MHC restricted. Nature 292, 547–549.

Kang SW, Rane NS, Kim SJ, Garrison JL, Taunton J, Hegde RS (2006). Substrate-specific translocational attenuation during ER stress defines a pre-emptive quality control pathway. Cell 127, 999–1013.

Karapetyan YE, Sferrazza GF, Zhou M, Ottenberg G, Spicer T, Chase P, Fallahi M, Hodder P, Weissmann C, Lasmezas CI (2013). Unique drug screening approach for prion diseases identifies tacrolimus and astemizole as antiprion agents. Proc Natl Acad Sci USA 110, 7044–7049.

Knowles TP, Waudby CA, Devlin GL, Cohen SI, Aguzzi A, Vendruscolo M, Terentjev EM, Welland ME, Dobson CM (2009). An analytical solution to the kinetics of breakable filament assembly. Science 326, 1533–1537.

Liang J, Kong Q (2012). alpha-Cleavage of cellular prion protein. Prion 6, 453–460.

Lietman CD, Rajagopal A, Homan EP, Munivez E, Jiang MM, Bertin TK, Chen Y, Hicks J, Weis M, Eyre D, et al. (2014). Connective tissue alterations in Fkbp10-/- mice. Hum Mol Genet 23, 4822–4831.

Lilley BN, Ploegh HL (2004). A membrane protein required for dislocation of misfolded proteins from the ER. Nature 429, 834–840.

Liu J, Farmer JD Jr, Lane WS, Friedman J, Weissman I, Schreiber SL (1991). Calcineurin is a common target of cyclophilin-cyclosporin A and FKBP-FK506 complexes. Cell 66, 807–815.

Mallucci G, Dickinson A, Linehan J, Klohn PC, Brandner S, Collinge J (2003). Depleting neuronal PrP in prion infection prevents disease and reverses spongiosis. Science 302, 871–874.

Masel J, Jansen VA, Nowak MA (1999). Quantifying the kinetic parameters of prion replication. Biophys Chem 77, 139–152.

Mays CE, Joy S, Li L, Yu L, Genovesi S, West FG, Westaway D (2012). Prion inhibition with multivalent PrPSc binding compounds. Biomaterials 33, 6808–6822.

Mays CE, Kim C, Haldiman T, van der Merwe J, Lau A, Yang J, Grams J, Di Bari MA, Nonno R, Telling GC, et al. (2014). Prion disease tempo determined by host-dependent substrate reduction. J Clin Invest 124, 847–858.

Miao M, Reichheld SE, Muiznieks LD, Huang Y, Keeley FW (2013). Elastin binding protein and FKBP65 modulate in vitro self-assembly of human tropoelastin. Biochemistry 52, 7731–7741.

Mukherjee A, Morales-Scheihing D, Gonzalez-Romero D, Green K, Taglialatela G, Soto C (2010). Calcineurin inhibition at the clinical phase of prion disease reduces neurodegeneration, improves behavioral alterations and increases animal survival. PLoS Pathog 6, e1001138.

Nakagaki T, Satoh K, Ishibashi D, Fuse T, Sano K, Kamatari YO, Kuwata K, Shigematsu K, Iwamaru Y, Takenouchi T, et al. (2013). FK506 reduces abnormal prion protein through the activation of autolysosomal degradation and prolongs survival in prion-infected mice. Autophagy 9, 1386–1394.

Ong DS, Wang YJ, Tan YL, Yates JR 3rd, Mu TW, Kelly JW (2013). FKBP10 depletion enhances glucocerebrosidase proteostasis in Gaucher disease fibroblasts. Chem Biol 20, 403–415.

Orsi A, Sitia R (2007). Interplays between covalent modifications in the endoplasmic reticulum increase conformational diversity in nascent prion protein. Prion 1, 236–242.

Priola SA, McNally KL (2009). The role of the prion protein membrane anchor in prion infection. Prion 3, 134–138.

Prusiner SB (1982). Novel proteinaceous infectious particles cause scrapie. Science 216, 136–144.

Prusiner SB, McKinley MP, Bowman KA, Bolton DC, Bendheim PE, Groth DF, Glenner GG (1983). Scrapie prions aggregate to form amyloid-like birefringent rods. Cell 35, 349–358.

Rane NS, Yonkovich JL, Hegde RS (2004). Protection from cytosolic prion protein toxicity by modulation of protein translocation. EMBO J 23, 4550–4559.

Rutkevich LA, Cohen-Doyle MF, Brockmeier U, Williams DB (2010). Functional relationship between protein disulfide isomerase family members during the oxidative folding of human secretory proteins. Mol Biol Cell 21, 3093–3105.

Rutkevich LA, Williams DB (2012). Vitamin K epoxide reductase contributes to protein disulfide formation and redox homeostasis within the endoplasmic reticulum. Mol Biol Cell 23, 2017–2027.

Sun S, Shi G, Han X, Francisco AB, Ji Y, Mendonca N, Liu X, Locasale JW, Simpson KW, Duhamel GE, et al. (2014). Sel1L is indispensable for mammalian endoplasmic reticulum-associated degradation, endoplasmic reticulum homeostasis, and survival. Proc Natl Acad Sci USA 111, E582–E591.

Trevitt CR, Collinge J (2006). A systematic review of prion therapeutics in experimental models. Brain 129, 2241–2265.

Voigt S, Jungnickel B, Hartmann E, Rapoport TA (1996). Signal sequence-dependent function of the TRAM protein during early phases of protein transport across the endoplasmic reticulum membrane. J Cell Biol 134, 25–35.

White MD, Farmer M, Mirabile I, Brandner S, Collinge J, Mallucci GR (2008). Single treatment with RNAi against prion protein rescues early neuronal dysfunction and prolongs survival in mice with prion disease. Proc Natl Acad Sci USA 105, 10238–10243.

Xiao J, Nie A, Li S (2007). Evaluation of neuroimmunophilin ligands. In: Drug Discovery Research: New Frontiers in the Post-Genomic Era, ed. Z Huang, Hoboken, NJ: Wiley, 203–229.

Ye Y, Shibata Y, Yun C, Ron D, Rapoport TA (2004). A membrane protein complex mediates retro-translocation from the ER lumen into the cytosol. Nature 429, 841–847.

Ziegler A, Uchanska-Ziegler B, Zeuthen J, Wernet P (1982). HLA antigen expression at the single cell level on a K562 X B cell hybrid: an analysis with monoclonal antibodies using bacterial binding assays. Somatic Cell Genet 8, 775–789.